Journal of Molecular Liquids 273 (2019) 392–407

Contents lists available at ScienceDirect

Journal of Molecular Liquids

journal homepage: www.elsevier.com/locate/molliq

Tautomerism, solvatochromism, preferential solvation, and density functional study of some heteroarylazo dyes

A. Ghanadzadeh Gilani [a,*], V. Taghvaei [a], E. Moradi Rufchahi [b], M. Mirzaei [c]

[a] Physical chemistry Lab., Department of Chemistry, University of Guilan, Rasht, Iran
[b] Department of Chemistry, Faculty of Science, Lahijan Branch, Islamic Azad University, Lahijan, Iran
[c] Bioinformatics Research Center, School of Pharmacy and Pharmaceutical Sciences, Isfahan University of Medical Sciences, Isfahan, Iran

ARTICLE INFO

Article history:
Received 4 August 2018
Received in revised form 25 September 2018
Accepted 11 October 2018
Available online 15 October 2018

Keywords:
Heteroarylazo dye
Azo-hydrazone tautomerism
Solvatochromism
Acid-base equilibrium
Preferential solvation
TD-DFT calculation

ABSTRACT

Photophysical characteristics of four synthesized heteroarylazo quinoline dyes were studied in various media with different solvatochromic parameters. Preferential solvation of the compounds was investigated in some mixed binary solvents. It was established that in the media with basic nature, only one tautomeric form and corresponding anion exist, which the latter is the main species. In the polar protic solvent, both the azo and hydrazone forms are present. The linear solvation energy relationships (LSER) were used to correlate the absorption spectral data. Using the absorption and emission spectra, the ground and the excited states dipole moments of the compounds were evaluated. The dyes were observed to show halochromism, dichromism, and anion affinity as well. The acid-base equilibria between neutral and anionic forms of the compounds were studied in buffer solutions of varying pH and ionization constants for these dyes were determined. The dyes exhibit positive linear dichroic behavior in the anisotropic medium, which indicate that all the absorption bands are due to the $\pi - \pi^*$ transitions. In order to analysis of the spectral behavior, time-dependent density functional theory (TD-DFT) calculations were performed.

1. Introduction

Due to the development of science and technology, synthetic azo dyes have found increasing applications in various fields such as laser, ink-jet printers, optical data storage, sensitized solar cells, non-linear optics and biological systems [1–6]. Moreover, a number of azo dyes are used in textiles, cosmetics, and drugs industries [7].

The design and development of new azo compounds having heterocyclic moieties with high tinctorial strength and brightness properties become popular in recent years [8]. Recently many azo dyes having quinoline moiety as coupling component have been synthesized and reported in the literature [9–12]. Although, the structure of these coloring materials is well defined, synthesis and development of new heteroarylazo quinoline compounds having stability and interesting photo-physical properties are needed in a large range of industrial and scientific applications. Thus, the knowledge of the spectroscopic data and the influence of molecular structure on the photo-physical behavior of theses coloring materials are always required.

As the photo-physical performance of the azo-hydrazone dyes is strongly related to their tautomeric equilibria and structural parameters, the study of the azo-hydrazone tautomerism is one of the most interesting fields in structural chemistry [13–23]. This phenomenon is very sensitive to environmental conditions such as temperature, dye concentration, solvent nature, pH, presence of additives, and others [24–26]. The environment characteristic is very important issue in formation and stability of the tautomers in solutions [27]. The azo-hydrazone equilibrium and intra-molecular hydrogen transfer is strongly related to the nature of intermolecular interactions. Polar media are best for formation and stability of hydrazone tautomer as well as electron-withdrawing substituents [23].

The solvatochromic shifts of the absorption and emission maxima in various environments present a reliable method to evaluate ground- and excited-state dipole moment. This technique is based on linear correlation between the absorption and emission maxima wave numbers and solvent polarity function [28,29]. The Lippert-Mataga [30], Bakhshiev [31] and Kawski–Chamma–Viallet [32] are among the most used solvent polarity functions. The solvatochromic data can also be used for quantitative estimation of the contribution of various types of dye–solvent interactions using the Katritzky and Kamlet–Taft multiparameter polarity scales [33].

Moreover, preferential solvation (PS) study was carried out on the absorption spectra of the compounds in three different binary solvent mixtures (toluene-methanol, DMSO-methanol, and acetic acid-DMF). It is a valuable method for characterizing and understanding the dye-

* Corresponding author at: Physical Chemistry Lab., Department of Chemistry, Faculty of Science, University of Guilan, 41335 Rasht, Iran.
E-mail address: aggilani@guilan.ac.ir (A. Ghanadzadeh Gilani).

https://doi.org/10.1016/j.molliq.2018.10.054
0167-7322/

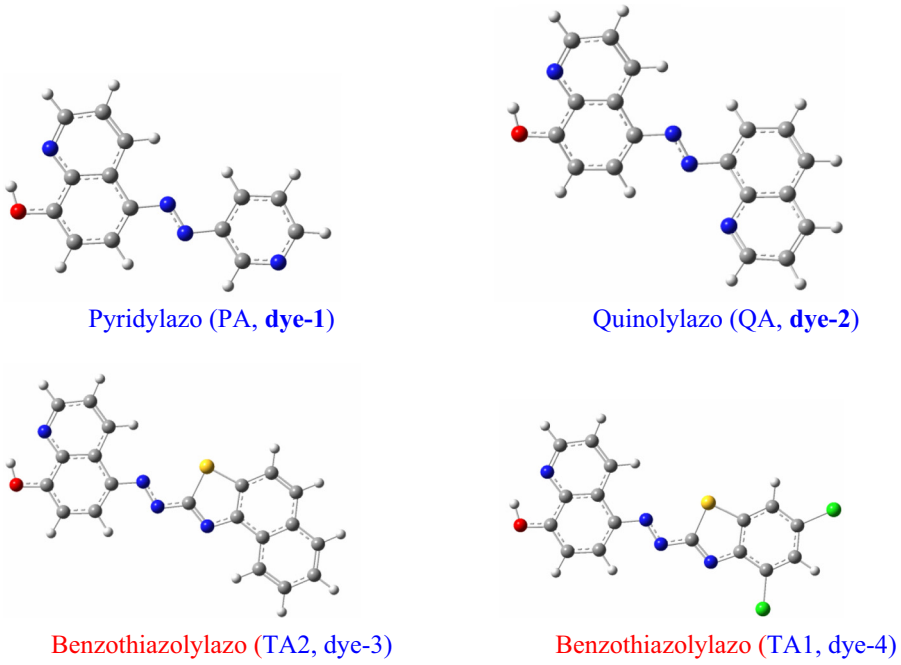

Fig. 1. Molecular structures of heteroarylazo quinoline dyes.

solvent interactions in the liquid mixture [34]. However, the dye–solvent interaction is more complex in mixed than in pure solvents. In addition, the spectral features of azo dyes in ordered nematic liquid crystals as anisotropic media are strongly influenced by anisotropic intermolecular interaction [35]. Compared to traditional spectra, polarized absorption spectra provide additional information on the optical properties, direction of transition moment, and dichroism of these compounds.

As a continuation of our research programs towards future understanding the nature of interactions and effective factors on spectral and structure characteristics of the azo quinoline dyes [10,27], we present the absorption and emission spectra along with solvatochromic and tautomeric behavior of four heteroarylazo quinoline compounds (Fig. 1).

The main idea behind our investigation is to characterize effects of the different type of molecular interactions and intra-molecular hydrogen transfer on the spectral performance of the synthesized dyes. Moreover, effect of the different heterocyclic rings (pyridyl, quinolyl, benzothiazolyl) on the spectral data and azo/hydrazone tautomerism were studied. On the other hand, this study is concerned with the evaluation of the ground- and excited state dipole moments of the dyes using different models [30–32]. The solvatochromic data were also used to analyze the solute–solvent interactions using correlation of the multi-parameter polarity scales. We show that the dyes exhibit both the halochromic and anion affinity effects. Deprotonation process and acid-base equilibrium for these dyes were investigated in ethanol-water media. Polarized absorption spectra of the dyes in a nematic solvent were measured and analyzed to obtain valuable information on the directions of the electronic transition dipole moments relative to the molecular axes [36]. Finally, time-dependent density functional theory (TD-DFT) calculations were performed for the dyes.

2. Experimental

2.1. Materials and apparatus

All the organic chemicals and solvents used for the synthesis and spectroscopic properties of the heteroarylazo dyes were of reagent or spectroscopic grades and purchased from Merck, Sigma–Aldrich, and Fluka. The organic solvents were used directly as supplied without any further purification. Their physical properties along with their polarity parameters [33] are listed in Table 1. In this research, a nematic liquid crystal (pentyl cyanobiphenyl, 5CB) was used as anisotropic solvent. The nematic compound was obtained from the military technical academy, Warsaw, Poland.

Melting points were determined with a Barnstead Electrothermal 9100 melting point apparatus in open capillary tubes and uncorrected. ^{1}H and ^{13}C NMR spectra measured on a Bruker 400 MHz spectrometer in DMSO-d_6 and $CDCl_3$ using TMS as an internal reference. Elemental analyses were performed at the Micro analytical Center using Eager 300 for EA1112 Elemental Analyzers and the results were within the accepted range of the calculated values. The absorption spectra of the compounds were scanned on a Cary UV–vis Double-beam spectrophotometer (Model 100). Fourier transformation infrared spectra (in KBr pellets) were recorded on a Shimadzu-8400 FT-IR spectrometer. Microanalyses for C, H and N were performed on a Perkine Elmer 2400(II) elemental analyzer.

Table 1
The solvatochromic parameters (α, β, and π*), $E_T(30)$-values, permittivity (ε), and refractive index (n_D) for the solvents used [33].

Solvent	ε	n_D	α	β	π*	$E_T(30)$
n-Heptane	1.92	1.39	0.00	0.00	0.08	31.1
Cyclohexane	2.02	1.43	0.00	0.00	0.00	30.9
1,4-Dioxane	2.21	1.42	0.00	0.37	0.49	36.0
Toluene	2.38	1.50	0.00	0.11	0.49	33.9
Chloroform	4.89	1.45	0.20	0.10	0.69	39.1
Acetic acid	6.17	1.37	1.12	0.45	0.64	51.7
THF	7.58	1.41	0.0	0.55	0.55	37.4
1-Octanol	10. 3	1.43	0.77	0.81	0.40	48.1
1-Heptanol	11.30	1.42	0.64	0.96	0.39	48.5
1-Hexanol	13.30	1.34	0.80	0.84	0.40	48.8
1-Pentanol	13.9	1.41	0.84	0.86	0.40	49.1
1-Butanol	17.51	1.39	0.84	0.84	0.47	49.7
2-Propanol	19.92	1.38	0.76	0.84	0.48	48.4
Acetone	20.56	1.36	0.08	0.48	0.62	42.2
Ethanol	24.55	1.36	0.86	0.75	0.54	51.9
Methanol	32.66	1.33	0.98	0.66	0.60	55.4
DMF	36.71	1.42	0.00	0.69	0.88	43.2
DMSO	46.45	1.48	0.00	0.76	1.00	45.1

2.2. Sample preparation

Stock solutions of each synthesized dyes (1×10^{-3} M) was prepared by mass and dissolved in an appropriate amount of dimethyl sulfoxide (spectroscopy grade) in 25 ml volumetric flask at room temperature. The sample solutions with proper concentrations were made using a Brand Transferpette micropipette and aliquot of the stock solutions. The sample weighing was carried out using an electronic analytical balance (AND model HR-200) with an accuracy of ±0.1 mg.

2.3. Buffer preparation and pH measurement

The buffer solutions for the pH range from 1 to 13 were prepared as given details elsewhere [37]. The chemicals used for the buffer solutions were analytical grade and obtained from Merck and Aldrich. The common composition and the corresponding pH values of buffer solutions are summarized in Supplementary data Table 1.

A digital pH meter Genway model 3505 was applied to measurement of the pH values. The pH meter readings in 50 vo1% ethanol-water solutions were corrected into pH values using the widely used relation of Van Uitert and Haas equation [38]

$$\left[-\log\left[H^{+}\right] = B + \log U_H\right] \quad (1)$$

where $\log U_H$ is the correction factor and B is pH meter reading. The readings were carried out at room temperature on a series of solutions with known quantities of HCl and NaOH in which the ionic strength was equal to 0.1 in 50 vol% ethanol-water mixture. The pK_a values were calculated using the following equation;

$$pK_a = pH_i + \log[(A_b\text{-}A_i)/(A_i - A_a)] \quad (2)$$

where A_i is the absorbance of the solution at intermediate pH_i and A_a and A_b are the absorbance values of the strongest acidic and basic buffer solutions.

2.4. Absorption and fluorescence spectra measurements

The absorption spectra of the synthesized dyes were recorded using a Cary 100 UV–vis double-beam spectrophotometer at room temperature. The absorption maxima of the azo and hydrazone tautomers were evaluated using an Origin's peak analysis program. This program allowed a more precise estimation of the peak profile. The spectrophotometer base line was calibrated against a solvent and was zeroed with a blank. The uncertainty in measured wavelength of absorption maximum was ±0.1 nm. Fluorescence spectra of the compounds in liquid solutions were recorded on a Shimadzu RF5000 spectrofluorimeter at room temperature. In order to avoid self-absorption process, the emission spectra were recorded in dilute solutions of the dyes.

2.5. Polarized absorption spectra measurements

Polarized absorption measurements [36] were carried out for the compounds in pentyl cyanobiphenyl (5CB) with planar orientation using the spectrophotometer equipped with polarizers. Dichroic ratio ($A_{//}/A_{\perp}$) of the dyes were determined based on the measurements of parallel ($A_{//}$) and perpendicular ($A_{\perp}$) absorbances to nematic direction (the rubbing direction of the cell).

2.6. Preparation of heteroarylazo dyes ***1–4***

Four heteroarylazo quinoline dyes were synthesized by conventional diazo coupling reaction of amino benzothiazolyl derivatives as diazo components [8]. This is followed by a brief description of the procedure used to prepare these compounds:

Heterocyclic amines (2.0 mmol) were dissolved in glacial acetic acid-propionic acid mixture (2:1, 6 mL) and cooled to 0–5 °C in an ice-salt bath. Then, a cold solution of nitrosyl-sulfuric acid, prepared from sodium nitrite (2 mmol, 0.15 g) and concentrated sulfuric acid (4 mL at 70 °C), was added drop wise to this liquor over a period of 20–30 min. The solution turned yellow, indicating the formation of diazonium salt, and left stirring for further 2 h at 0–5 °C. Afterwards, the diazonium salt liquor was added slowly to a vigorously stirred solution of 8-hydroxyquinoline (2 mmol, 0.29 g) in ethanol-water mixture (1:4, 5 mL) containing sodium hydroxide (5 mmol, 0.2 g). The resulting solution was vigorously stirred at 0–4 °C for 2 h, while the pH of the reaction mixture was regulated at 5–6 by simultaneous addition of sodium hydroxide solution (0.5 M). The progress of the reaction was monitored by thin layer chromatography (TLC) and then crude dyes were filtered, washed with cold ethanol and purified by recrystallization method. The physical and spectral data of the purified dyes are shown below;

2.6.1. 5-(3-pyridylazo)-8-hydroxyquinoline (1)

Clear red crystals (Yield: 84%, Mp: 215–218 °C, Reported 210 °C [8]); FT-IR (KBr): ν (cm^{-1}) =3216(br, OH), 1638(C=N), 1505(N=N), 1383(C—O); ^{1}H NMR (400 MHz, DMSO-d_6); δ 11.23 (1H, br, OH), 9.35(1H, dd, J = 8.4, 1.6 Hz) 9.19(1H, d, J = 2 Hz), 9.0(1H, dd, J = 4.4, 1.6 Hz), 8.72(1H, dd, J = 4.8, 1.2 Hz), 8.34(1H, dt, J = 8.4, 1.6 Hz), 8.02(1H, d, J = 8.8 Hz), 7.78(1H, 1H, dd, J = 8.4, 4.4 Hz), 7.63 (1H, dd, J = 8.4, 4.8 Hz), 7.26(1H, d, J = 8.8 Hz) ppm. ^{13}C NMR (100 MHz, DMSO-d_6) δ: 160.13, 159.15, 155.21, 153.13, 143.57, 140.43, 137.42, 137.10, 131.24, 127.32, 123.83, 122.44, 117.28, 112.25. Anal. Calcd. for $C_{14}H_{10}N_4O$: C, 67.19; H, 4.03; N, 22.39; Found: C, 67.71; H, 4.07, N, 22.47.

2.6.2. 5-(8-quinolylazo)-8-hydroxyquinoline (2)

Red crystals (Yield = 67%, Mp: 223–226 °C); FT-IR (KBr): ν (cm^{-1}) = 3200–3100 (br, OH), 1646 (C=N), 1501(N=N), 1348 (C—O); ^{1}H NMR (400 MHz, DMSO-d_6); δ 9.41 (1H, m), 9.1 (1H, d, J = 2.4 Hz), 9.01 (1H, d, J = 2.8 Hz), 8.52 (1H, dd, J = 8.2, 1.6 Hz), 8.18 (2H, m, overlapped), 7.97 (1H, d, J = 7.2 Hz), 7.82–7.75 (2H, m, overlapped), 7.70 (1H, dd, J = 8.2, 4.4 Hz), 7.30 (1H, d, J = 7.2 Hz) ppm. ^{13}C NMR (100 MHz, DMSO-d_6) δ: 158.36, 151.54, 149.54, 144.03, 140.20, 138.46, 136.78, 136.51, 132.48, 131.01, 129.25, 127.82, 127.18, 123.90, 122.64, 116.86, 116.33, 112.15. Anal. Calcd. for $C_{18}H_{12}N_4O$: C, 71.99; H, 4.03; N, 18.66; Found: C, 71.82; H, 4.09, N, 17.83.

2.6.3. 5-(2-naphtho [2,1-d]thiazolylazo)-8-hydroxyquinoline (3)

Red crystals (Yield = 70%, Mp:234–236 °C); FT-IR (KBr): ν (cm^{-1}) = 3420 (br, OH), 1617(C=N), 1542 (N=N), 1383(C—O); ^{1}H NMR (400 MHz, DMSO-d_6); δ 8.90 (1H, dd, J = 4.6, 2 Hz), 8.58(1H, dd, J = 8.4, 1.6 Hz), 8.51–8.49(2H, m, overlapped), 8.31 (1H, d, J = 8.0 Hz), 8.11–8.08(2H, m, overlapped), 7.79–7.68(3H, m, overlapped), 6.76(1H, d, J = 10.0 Hz) ppm. ^{13}C NMR (100 MHz, DMSO-d_6) δ: 163.18, 154.21, 153.89, 152.03, 145.01, 143.13, 138.16, 136.81, 136.55, 131.35, 129.14, 128.18, 127.09, 127.16, 128.10, 124.14, 121.24, 115.43, 114.65113.12.

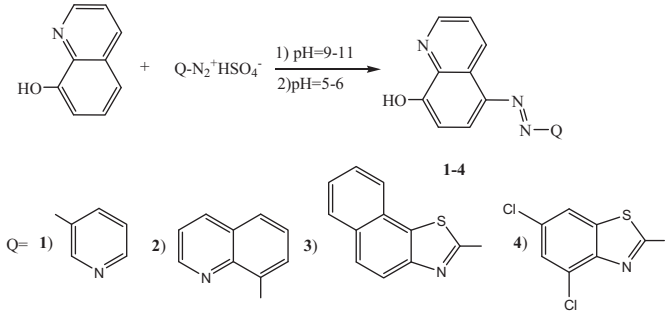

Scheme 1. Synthesis of heteroarylazo quinoline dyes **1–4**.

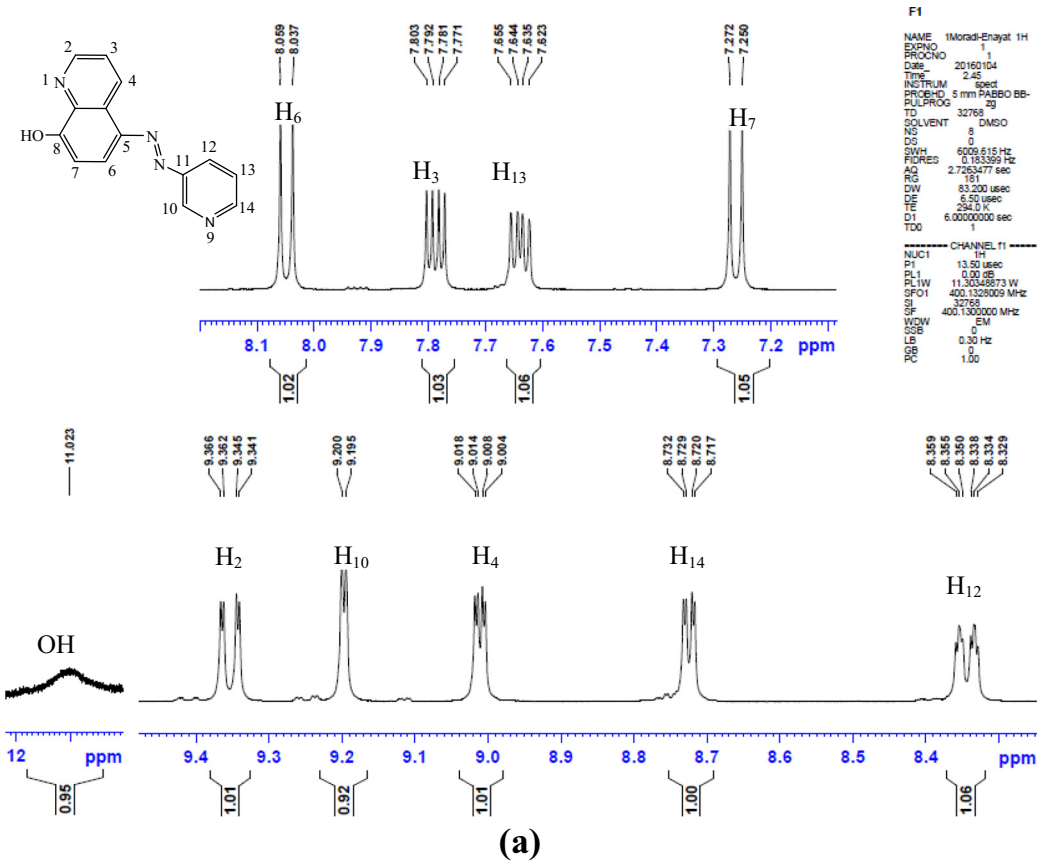

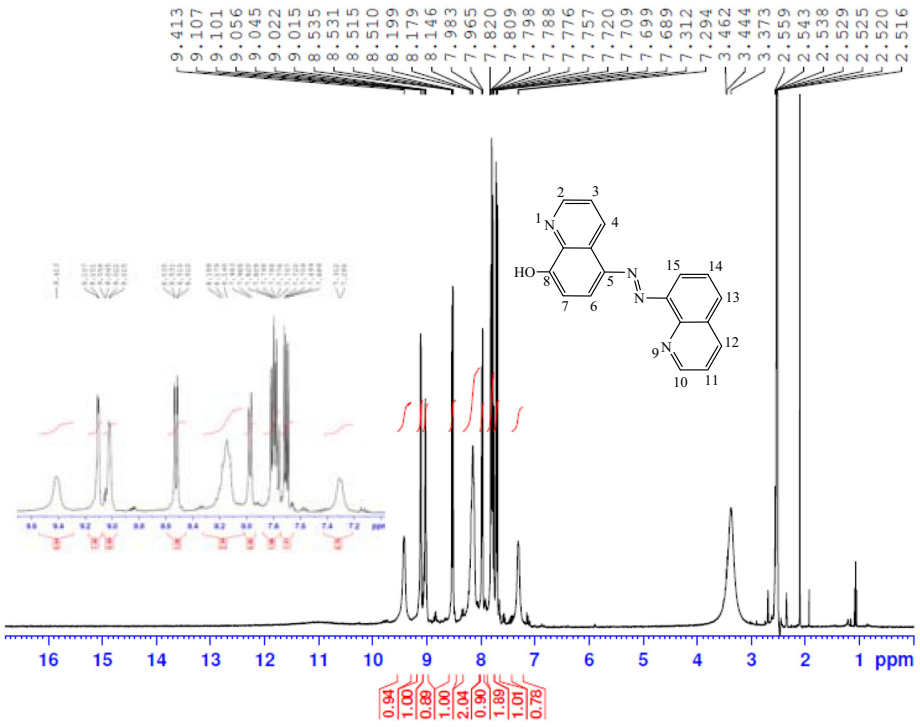

Fig. 2. (**a**) ^{1}H NMR spectrum of the dye **1**, (**b**) ^{1}H NMR spectrum of the dye **2** in DMSO-d_6 at 25 °C.

Anal. Calcd. for $C_{20}H_{12}N_4OS$: C, 67.40; H, 3.39; N, 15.72; S, 9.00; Found: C, 67.97; H, 3.45, N, 14.97.

2.6.4. 5-(4,6-dichlorobenzothiazolylazo)-8-hydroxyquinoline (4)

Violet crystals (Yield = 78%, mp > 300 °C), FT-IR (KBr): ν (cm^{-1}) = 3450 (OH), 1619 (C=N), 1503(N=N), 1134(C—O), 616 (C—Cl); ^{1}HNMR (400 MHz, DMSO-d_6); δ= 9.8 (1H, dd, J = 8.8, 1.6 Hz), 8.9 (1H, m, overlapped), 8.51–8.33 (1H, m, overlapped), 8.21–7.82 (2H, m, overlapped), 7.42(1H, d, J = 8.0 Hz), 7.27 (1H, d, J = 8.0 Hz). ^{13}C NMR (100 MHz, DMSO-d_6) δ:148.89, 148.58, 142.23, 138.27, 137.22, 136.74, 133.37, 131.81, 128.74, 127.30, 125.97, 124.23, 123.74, 122.14, 118.86, 117.46. Anal. Calcd. for $C_{16}H_8Cl_2N_4OS$ C, 51.22; H, 2.15; N, 14.93; S, 8.54; Found: C, 51.59; H, 2.18; N, 15.77; S, 8.77.

3. Results and discussion

3.1. Synthesis and characterization

In continuation of our research programs towards synthesis and spectroscopic properties of novel aryl and heteroarylazo azoquinoline-8-ol dyes, we prepared the heteroarylazo quinoline dyes **1**–**4** by using some heterocyclic aromatic amines as diazotizing component. Except for 5-(3-pyridylazo)-8-hydroxyquinoline (dye 1), the three new heteroarylazo dyes were synthesized afterwards following the procedure described in section 2.6 for the first time. The pyridinylazo dye has been previously synthesized by Ertan and coworkers and published earlier [8].

As shown in Scheme 1, four heterocyclic disperse azo dyes were synthesized from the appropriate hetaryl diazonium salts under basic condition in ethanol-water mixture. The dyes were obtained in satisfactory yields and purified by recrystallization from ethanol.

The chemical structures of the newly synthesized compounds (Fig. 1) were confirmed with FT-IR, ^{1}H NMR, ^{13}C NMR, UV–vis spectroscopy, and elemental analysis. The spectral data for the dyes clearly supported the proposed structures. FT-IR spectrum of compounds **1**–**4** showed broad hydroxyl (OH) bands at 3450–3100 cm^{-1}. The intense peak at 1646–1617 cm^{-1} can be attributed to C=N ring stretching of quinoline nucleus. The presence of N=N group was observed at 1542–1501 cm^{-1} region. Detailed assignments of the protons are given in the experimental section.

The ^{1}H NMR spectra of the dyes **1** (PA) and **2** (QA) are typically shown in Fig. 2a and b, respectively. The ^{1}H NMR spectrum of 5-(3-pyridyazo)-8-hydroxyquinoline (PA) measured in DMSO-d_6 at 25 °C and as it is obvious in Fig. 2a, the protons belonging to the aromatic system were observed at the expected chemical shifts and integral values. The spectrum showed three doublet of doublet signals at δ = 9.35, 9.00 and 7.78 ppm corresponding to H_2, H_4, and H_3 of the quinoline nucleus, respectively.

Moreover, Two doublet signals at δ = 8.0 and 7.26 ppm can be attributed to H_6 and H_7 of quinoline ring. The spectrum also showed a doublet at 9.20 ppm for H_{10} of pyridine ring with *meta* coupling constant J = 2.0 Hz. Two doublet of doublet at δ 8.72 and 7.63 having J 4.8, *1.2* Hz and *8.2*, *4.8* Hz assigned to H_{14} and H_{13}, respectively. The doublet of triplet at 8.34 ppm is due to H_{12}, formed by coupling with both *meta* (H_{10} and H_{14}) and an *ortho* proton (H_{13}). The peak at 11.02 ppm (Hydroxyl group) confirmed the presence of azo tautomer of the compound in DMSO solvent. The ^{1}H NMR spectra of 5-(8-quinolylyazo)-8-hydroxyquinoline (QA) is presented in Fig. 2b. The chemical shifts and splitting pattern are consistence with the proposed structure of the dye. The ^{13}C NMR spectra and elemental analysis of the dye 2 and dye 4 were typically presented in the Supplementary information (Figs. S1–S6).

3.2. Solvatochromism and tautomerism

The absorption spectra of the prepared heteroarylazo dyes were recorded in several organic solvents with different polarity and nature. The spectroscopic data are summarized in Table 2. The spectra were recorded and examined in dilute solutions within a concentration range of 2×10^{-6} to 2×10^{-5} M. At this range of concentrations, the dye exists in

Table 2
The maximum absorption wavelengths of the heteroarylazo quinoline dyes in various solvents.

Solvent	Pyridylazo (PA)		Quinolylazo (QA)		Benzothiazolylazo-1 (TA1)			Benzothiazolylazo-2 (TA2)	
	λ_1	λ_2	λ_1	λ_2	λ_1	λ_2	λ_3	λ_1	λ_2
Non-polar									
n-Heptane	383.1	–	385.3	500.8	–	–	–	–	–
Cyclohexane	384.6	–	384.1	499.3	–	–	–	–	–
1,4-Dioxane	388.9	–	394.8	491.1	434.6	–	–	499.1	–
Toluene	387.1	–	393.3	488.1	453.4	–	–	476.1	–
Polar protic									
Methanol	390.6	473.3	407.7	497.9	472.9	548.4	–	–	576.3
Ethanol	393.2	491.7	409.9	500.1	475.8	546.1	–	–	563.7
1-Propanol	422.1	467.4	396.9	496.9	461.5	541.8	–	–	590.3
1-Butanol	407.9	485.4	415.2	495.5	416.4	548.6	–	–	562.6
1-Pentanol	413.5	458.7	405.5	495.8	419.3	551.9	–	–	565.5
1-Hexanol	396.8	488.3	405.4	497.6	–	567.9	–	–	558.9
1-Heptanol	395.6	476.2	407.4	497.9	–	530	–	–	556.3
1-Octanol	396.5	475.3	429.9	–	–	538	–	–	553.7
Acetic acid	396.9	485.2	418.2	497.7	488.4	–	–	486.7	–
1,5-pentanediol	398.8	–	408.9	–	453.7	553.3	–	–	576.2
Dipolar aprotic									
THF	391.2	487.6	406.3	489.6	–	539.1	562.8	–	559.7
Acetone	387.1	387.1	390.5	482.8	475.9	546.9	576.6	–	565.4
DMF	411.7	411.7	398.6	519.9	–	560.1	591.3	428.9	586.1
DMSO	398.6	398.6	401.3	507.5	–	560.8	597.3	426.7	589.2
Basic media									
Triton X-100	395.5	512.9	399.9	520.4	–	562.6	596.1	–	592.2
1-Methylimi dazole	412.9	527.9	416.2	434.6	–	561.1	597.5	–	589.9
AEEA	–	518.2	–	524.6	–	563.8	599.2	–	594.2
DEA	–	508.2	–	521.9	–	564.2	596.4	–	595.1
Water-ethanol/NaOH	–	501.8	–	505.5	–	557.8	591.1	–	596.6

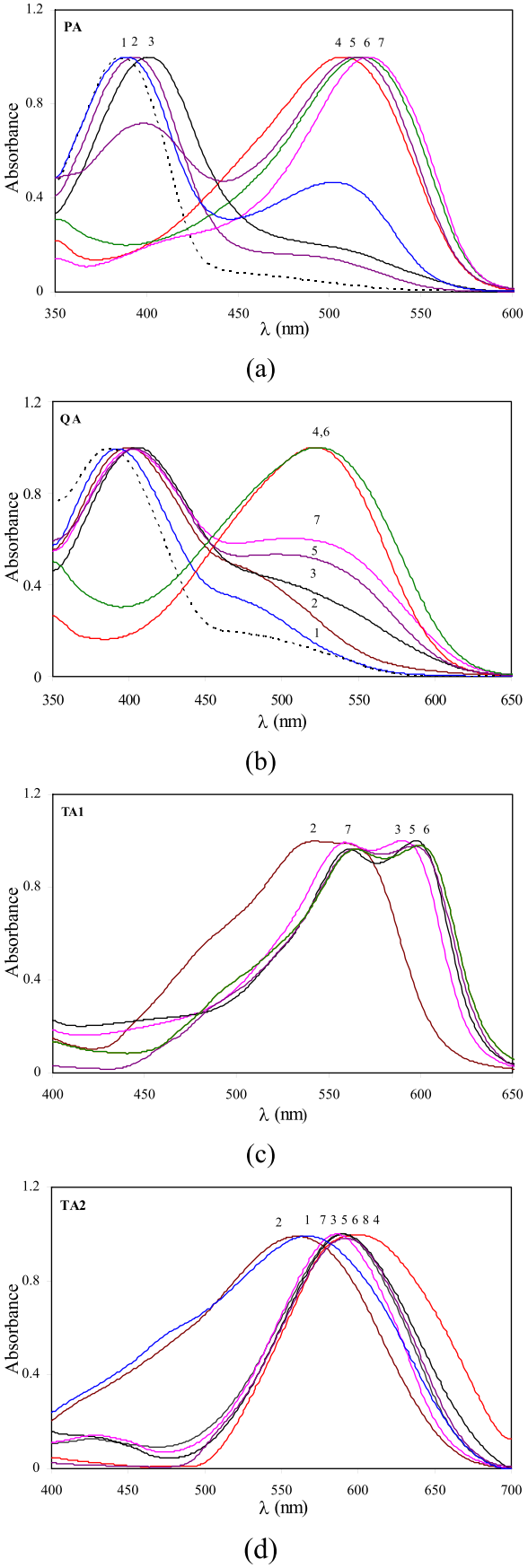

Fig. 3. Normalized absorption spectra of (a) pyridylazo (PA), (b) quinolylazo (QA), (c) benzothiazolylazo-1 (TA1), (d) benzothiazolylazo-2 (TA2) in dipolar aprotic and basic solvents: (1) acetone, (2) THF, (3) DMSO, (4) DEA, (5) TX-100, (6) AEEA, (7) DMF; (dashed spectrum is the absorbance of the dye in cyclohexane as reference solvent).

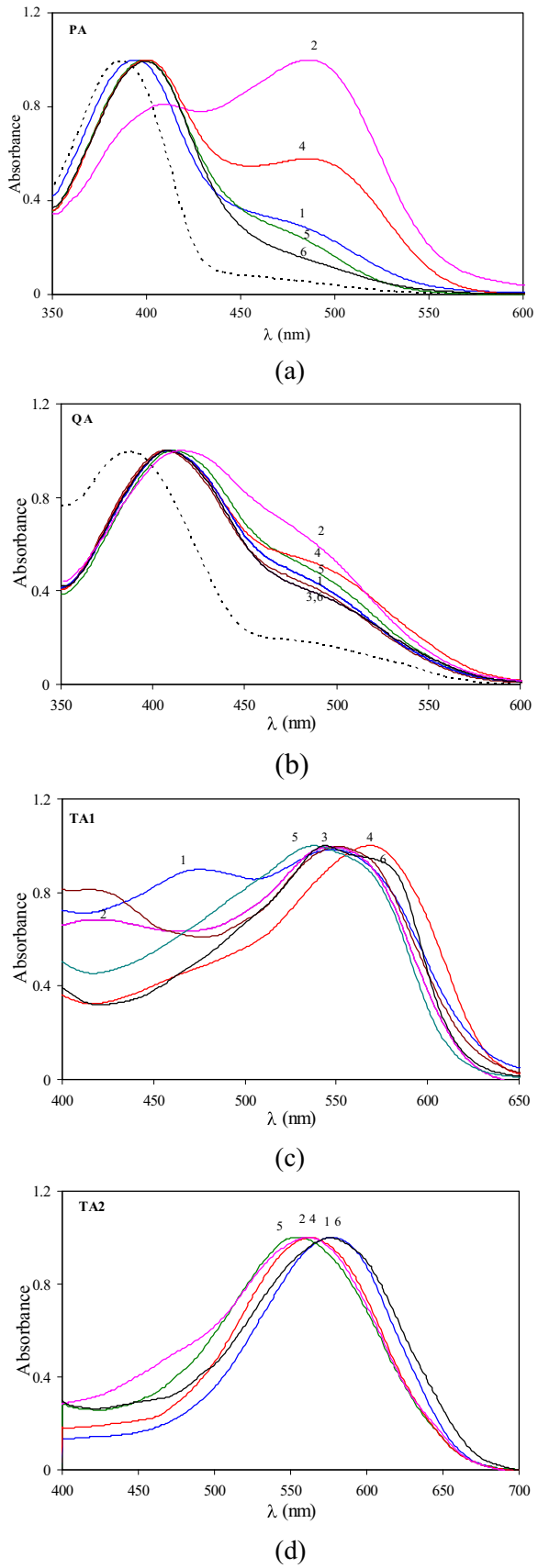

Fig. 4. Normalized absorption spectra of (a) pyridylazo (PA), (b) quinolylazo (QA), (c) benzothiazolylazo-1 (TA1), (d) benzothiazolylazo-2 (TA2) in alcoholic solvents: (1) methanol, (2) 1-butanol, (3) 1-pentaol, (4) 1-hexanol, (5) 1-octanol, (6) 1,5-pentanediol; (dashed spectrum is the absorbance of the dye in cyclohexane as reference solvent).

Table 3
Percentage of different parameters contributions for Kamlet–Taft multiparameter scale.

Dye	Form	α	β	π^*
Pyridylazo (PA)	Azo	15 (±9)	63 (±10)	22 (±8)
	Hydrazone	14(±5)	30(±14)	**57(±13)**
Quinolylazo (QA)	Azo	42 (±3)	15 (±6)	44 (±5)
	Hydrazone	20(±4)	21(±7)	**59(±6)**
Benzothiazolylazo (TA1)	Azo	2 (±0)	4 (±1)	94 (±2)
	Hydrazone	29(±4)	32(±11)	**39(±6)**
Benzothiazolylazo (TA2)	Azo	5 (±9)	23 (±8)	71 (±17)
	Hydrazone	22 (±7)	14 (±9)	**64 (±8)**

solution almost entirely in the monomeric form. In this work, no evidence was found for their self-association at the low concentrations. Fig. 3(a–d) typically presents visible absorption spectra of the dyes in selected organic media mainly dipolar aprotic solvents. As can be observed, the environment has profound effects on the spectral characteristics of the synthesized compounds. All the dyes in a reference solvent, i.e. cyclohexane, show simple absorption band at shorter wavelengths due to the existence of the only one tautomeric azo form. On going from cyclohexane to the polar solvents, the absorption maximum of the dyes shows irregular spectral shifts that cannot be explained in terms of solvatochromic behavior. It seems that the spectral variation take place according to the basic strength of the media.

As shown in the figure, two, or even more, absorption peaks appear in the visible spectra of the heteroarylazo dyes in a number of used solvents. The question then appears what is the origin of the spectral characteristics for the synthesized dyes? There can be at least four possible explanations for the spectral behavior. The first explanation is based on formation of the two tautomers. This characteristic might be due to the azo-hydrazone tautomerism, where the absorption bands at longer wavelengths are due to the hydrazone form. The tautomerism is more obvious for the dyes dissolved in the polar solvents that the hydrazone form might be dominated in the dipolar aprotic solvents or the basic media. These groups of solvents induce to enhance medium basicity, and therefore, the azo form might be converted into another structure.

The second one involves the presence of neutral and anionic species, assumes the existence of the only one tautomeric form and its corresponding anionic species, which is more probable in the basic media. The presence of the anionic and neutral species in solutions can be involved in the dual spectral band of the dyes.

The third explanation highlights the possible simultaneously existence of the three structural species (azo, hydrazone, and anionic forms) in some cases, in particular for the benzothiazolylazo compound (TA1), where the absorption bands at longer wavelengths split into two peaks. This phenomenon could be attributed to co-existence of both hydrazone and anionic forms in the polar aprotic and multifunctional media. The absorptions of hydrazone and anionic forms are close to each others but in the higher wavelengths than those of azo form.

The fourth elucidation is only the anionic forms may be existed in water-ethanol-NaOH solutions and some media with basic nature such as diethanolamine (DEA), aminoethyl ethanol amine (AEEA), and 1-methylimidazole (1-MEM). The last case is more obvious for the other benzothiazolylazo compound (i.e. TA2).

Table 4
Percentage of different parameters contributions for Katritzky multiparameter scale.

Dye	Absorbance	$P_{E_T(30)}$(%)	$P_{\varepsilon,}$(%)	P_n(%)
Pyridylazo (PA)	azo	**71(±13)**	28 (±9)	2 (±6)
	hydrazone	27(±2)	**38 (±9)**	35(±7)
Quinolylazo (QA)	azo	**66 (±3)**	23 (±3)	11 (±2)
	hydrazone	17(±10)	**77(±8)**	6(±5)
Benzothiazolylazo (TA1)	azo	11 (±8)	34 (±10)	**55 (±12)**
	hydrazone	41(±8)	**46(±7)**	13 (±7)
Benzothiazolylazo (TA2)	azo	**60(±0)**	8(±0)	3 (±0)
	hydrazone	28(±12)	**46(±10)**	26(±11)

Table 5
Calculated ground- and excited-state dipole moments (μg and μe) in selected solvents.

Dye	Polarity function	Slope	R^2	μg (D)	μe (D)	Δμ (D)
Pyridylazo (PA)	Lippert-Mataga	2673.8	0.85	3.79	7.90	4.11
	Bakhshiev	921.7	0.90	3.79	6.21	2.42
	Kawski-Chamma-Viallet	−3350.6	0.92	3.79	8.40	4.61
Quinolylazo (QA)	Lippert-Mataga	−25,100.8	0.980	3.69	8.94	5.25
	Bakhshiev	−8436.2	0.932	3.52	10.84	7.32
	Kawski-Chamma-Viallet	−10,447.1	0.972	3.52	11.67	8.15
Benzothiazolyl azo (TA2)*	Lippert-Mataga	−9747.4	0.96	5.5	14.89	9.39
	Bakhshiev	−3283.5	0.97	5.1	11.47	6.37
	Kawski-Chamma-Viallet	−8510.2	0.95	5.5	14.28	8.78

*The data are listed for the hydrazone tautomer.

The organic bifunctional solvents, DEA, AEEA, 1-MEM with both the basicities and the presence of H-bond donor or acceptor groups, were used in this study. These solvents may give many possibilities to form different type of interactions. They may form hydrogen bonds directly with the dye molecules in different available sites. DEA is an amino alcohol which has one secondary amine and two primaries –OH groups. AEEA is a diamine with one primary amine, one secondary amine, and one primary hydroxyl group. 1-MEM is a heterocyclic organic base and is a derivative of imidazole. AEEA, DEA, and 1-MEM have a basic chemical nature with pK_b values around 4.5, 5.1, and 6.6, respectively [39,40]. As can be seen from Fig. 3, the spectral characteristics of the dyes, in particular TA1 and TA2 are strongly affected by these basic media. The obvious spectral performance is the disappearance of the azo spectral band and the occurrence of a hydrazone or anionic peaks at longer wavelengths.

The similarities of absorption spectra of the dye in the amino alcohols (DEA or AEEA) and in the water-ethanol-NaOH solution suggest that the alkaline nature of these solvents has a profound effect on the dye spectra rather than their alcoholic character due to the existence of the hydroxyl groups. This effect is mainly responsible for the spectra changes observed for the dyes, where the neutral form of the dye may be formed on alkaline media. The hydrazone (or anionic) form is almost totally dominated in the basic media. On the contrary, the azo species is dominated in acidic environment. Furthermore in 1-MEM as *a* weak base solvent, azo and hydrazone forms are co-existence, where the hydrazone form is predominant.

Fig. 4 (a–d) shows the absorption spectra of the dyes in alcoholic solutions. As it is obvious from the figure, quinolylazo (QA) exists mainly in the azo form, while pyridylazo (PA) exhibits the presence of both the azo and hydrazone tautomers. On the other hand, benzothiazolylazo dyes (TA1 and TA2) exist almost in hydrazone forms in the polar protic solvents (from methanol to 1-octanol). Further inspection of the figure shows that the spectral shape and location of the dyes in 1,5-pentanediol (1,5PD) are similar to that of 1-pentanol. The presence of the two nonadjacent –OH groups in this diol induce no noticeable changes in the dye spectra. In the 1,5PD molecules, one hydroxyl group may interact with the dye molecules but the second one more probably is involved in the self-association trough the H-bonding, leads to the formation of a network structure [41].

Likewise, the dye absorption maximum demonstrates irregular shifts that cannot be elucidated by the solvatochromic parameters. It was observed that the dyes are almost totally in the azo form in apolar solvents such as cyclohexane. As a result, the hydrazone form becomes more favor in the order of the solutions containing TA2 > TA1 > PA > QA.

3.3. The linear solvation energy relationships (LSER)

The Kamlet-Taft and Katritzky LSER approaches [42] were used for quantitative evaluation of the solvent effects;

$$\bar{\nu} = \bar{\nu}_o + a \cdot \alpha + b \cdot \beta + c \cdot \pi^* \quad (3)$$

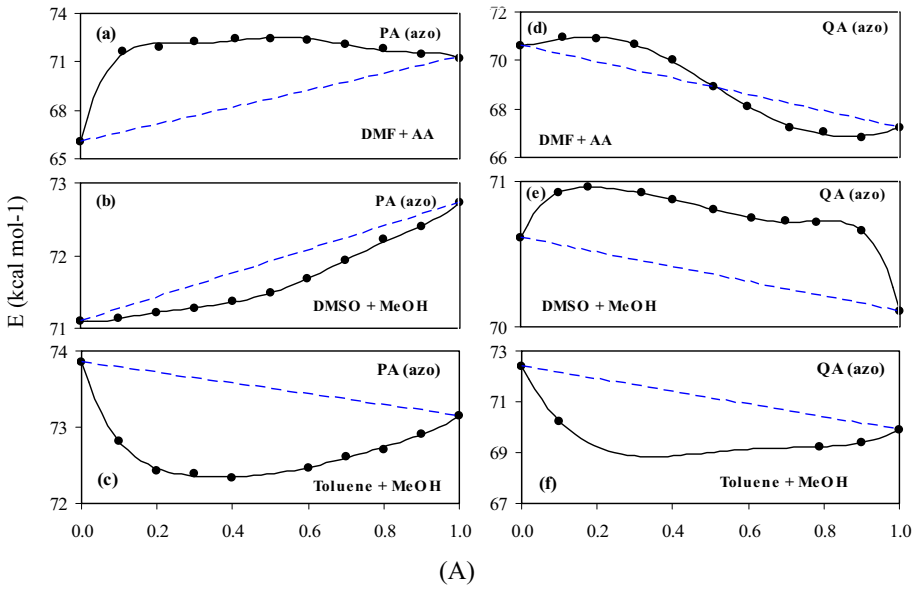

Fig. 5. Influence of the protic cosolvent on the E_{12} values for (a-c) pyridylazo (PA) and (d-e) quinolylazo (QA), in different binary solvents; DMF-acetic acid, DMSO- MeOH, and toluene-MeOH.

$$\bar{\nu} = \bar{\nu}_o + a \times E_T(30) + b \times (\varepsilon - 1/2\varepsilon + 1) + c \times (n^2 - 1/2n^2 + 1) \qquad (4)$$

$\bar{\nu}$ is the peak maximum in cm^{-1}. The *a*, *b*, and *c* coefficients are the relative susceptibilities of the solute property. The Kamlet-Taft solvent descriptors (Eq. 3), α, β, are the scales of solvent H-bond donor and acceptor abilities, respectively, and π^* is a measure of solvent dipolarity/polarizability. In the Katritzky equation (Eq. (4)), $E_T(30)$ is the Reichardt polarity function, ε is the dielectric constant, and *n* is the solvent refractive index.

The Kamlet-Taft equation estimates hydrogen bonding interactions between solute and solvent. The Katritzky equation evaluates the solvent dipolarity, polarizability, and specific interactions. The multi-parameter correlated values were determined using the solvent solvatochromic data (Table 1). The multi-linear regression analyses were carried out using the Excel 2010 package from the Microsoft and given in the Supplementary data Tables 2 to 5. The values obtained by the LSER models show a good regression fit to the experimental data.

In order to have comparable coefficients data, the parameters for all the used solvents were re-normalized and re-scaled and listed in Tables 3 and 4. Referring to the LSER correlations, the total involvement of the intermolecular interactions between the dye and the solvents was considered to be 100%. For the each correlation, it was divided for the various types of the interactions.

Referring to the Kamlet-Taft correlation, the solvent dipolarity/polarizability (π^*) have the main contribution into spectral characteristics of the benzothiazolylazo dyes (TA1 and TA2) in both the azo and hydrazone regions (Table 3). For the quinolyl and pyridyl dyes (PA and QA), the Kamlet-Taft correlation also shows that π^* has the major effectiveness in hydrazone region. However, the solvent hydrogen–bond donor and acceptor abilities (α, β) have almost main contribution into spectral characteristic of PA and QA in the azo region.

The Katritzky LSER model shows that values connected with the polarity, $E_T(30)$, and polarizability functions have the major effectiveness in azo region (Table 4). Meanwhile, for all the studied dyes, the polarity function (P_ε) has the major effectiveness in hydrazone region.

3.4. Preferential solvation

In order to deeper understand the influence of intermolecular interactions on the solvatochromic and tautomeric behavior of the dyes in

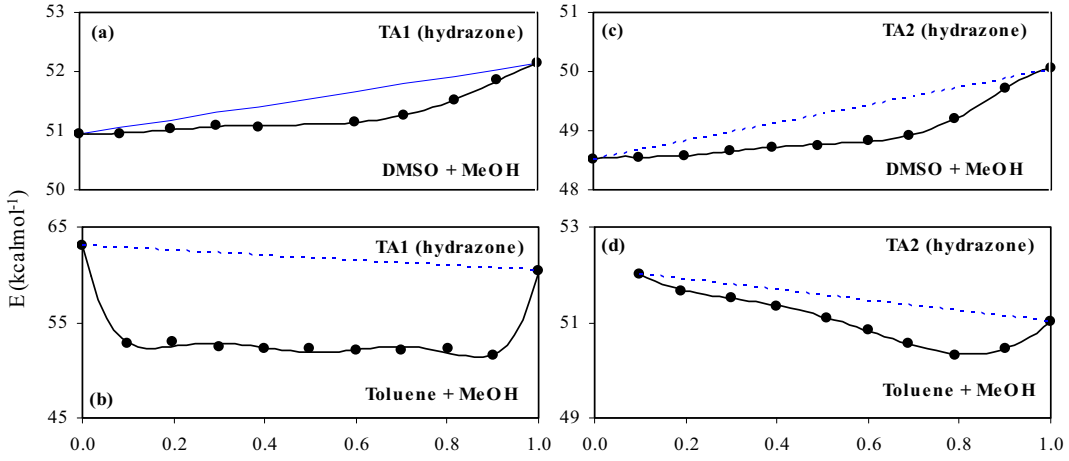

Fig. 6. Influence of the protic cosolvent on the E_{12} values for (a–b), benzothiazolylazo-1 (TA1), (c,d) benzothiazolylazo-2 (TA2), in the two binary mixed solvents; DMSO- MeOH, and toluene-MeOH.

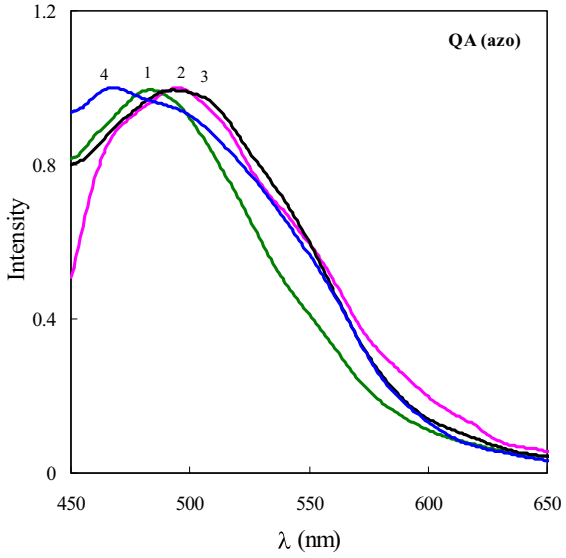

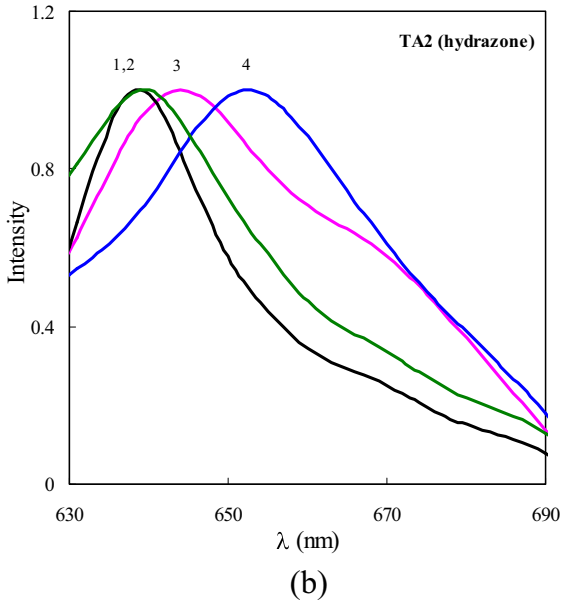

Fig. 7. Normalized emission spectra of (a) pyridylazo (PA) and (b) benzothiazolylazo-2 (TA2) in various solvents: 1) DMF, 2) 2-propanol, 3) DMSO, 4) ethanol.

this report; the preferential solvation was carried out. In a binary liquid solvent, a solute molecule can preferentially interact with one solvent rather than the other, which depends on the solute and the solvent nature and composition of the solvation microsphere (cybotatic region) [43,44].

The transition energy of maximum absorption (E) of the dyes was calculated from the following expression;

$$E_{12}/Kcalmol^{-1} = 28591/\lambda_{max} \quad (5)$$

For ideal solvation behavior, values of the transition energy of the dyes in mixed solvents were obtained using the equation;

$$E_{12}^{ideal} = x_1E_1 + x_2E_2 \quad (6)$$

where x_1 and x_2 represent the mole fractions of the pure solvent 1 and solvent 2. In two phase model of solvation, solvent molecules are

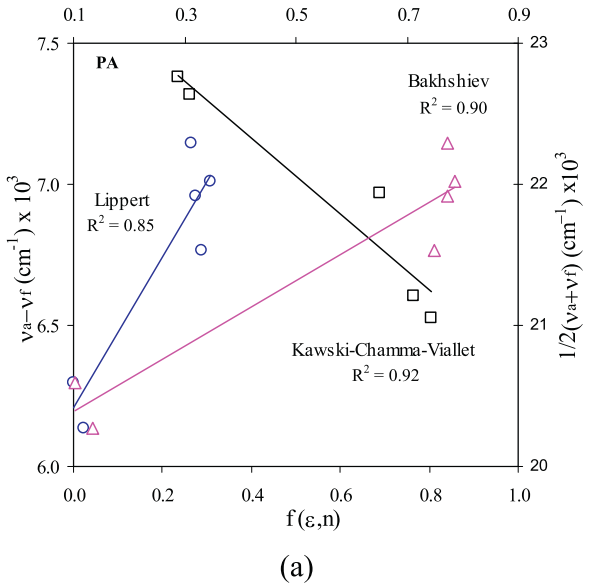

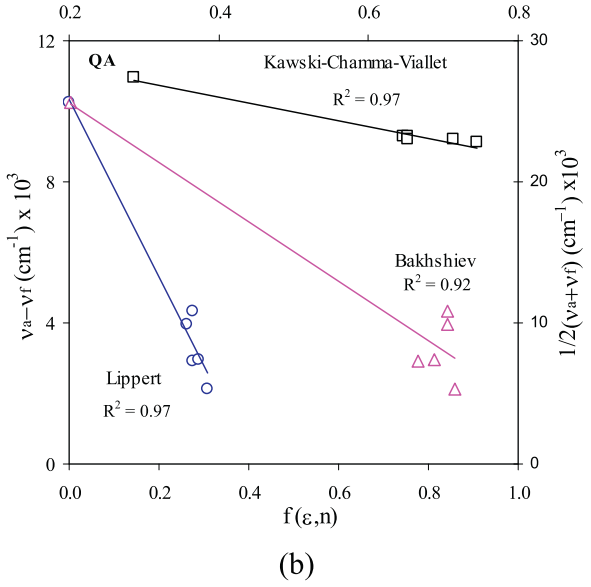

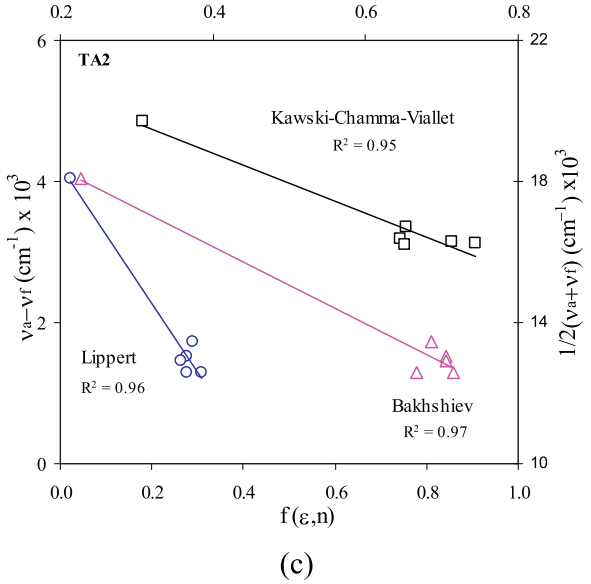

Fig. 8. Solvent polarity functions fitness; (a) pyridylazo (PA), (b) quinolylazo (QA), (c) benzothiazolylazo-2 (TA2) in selected solvents.

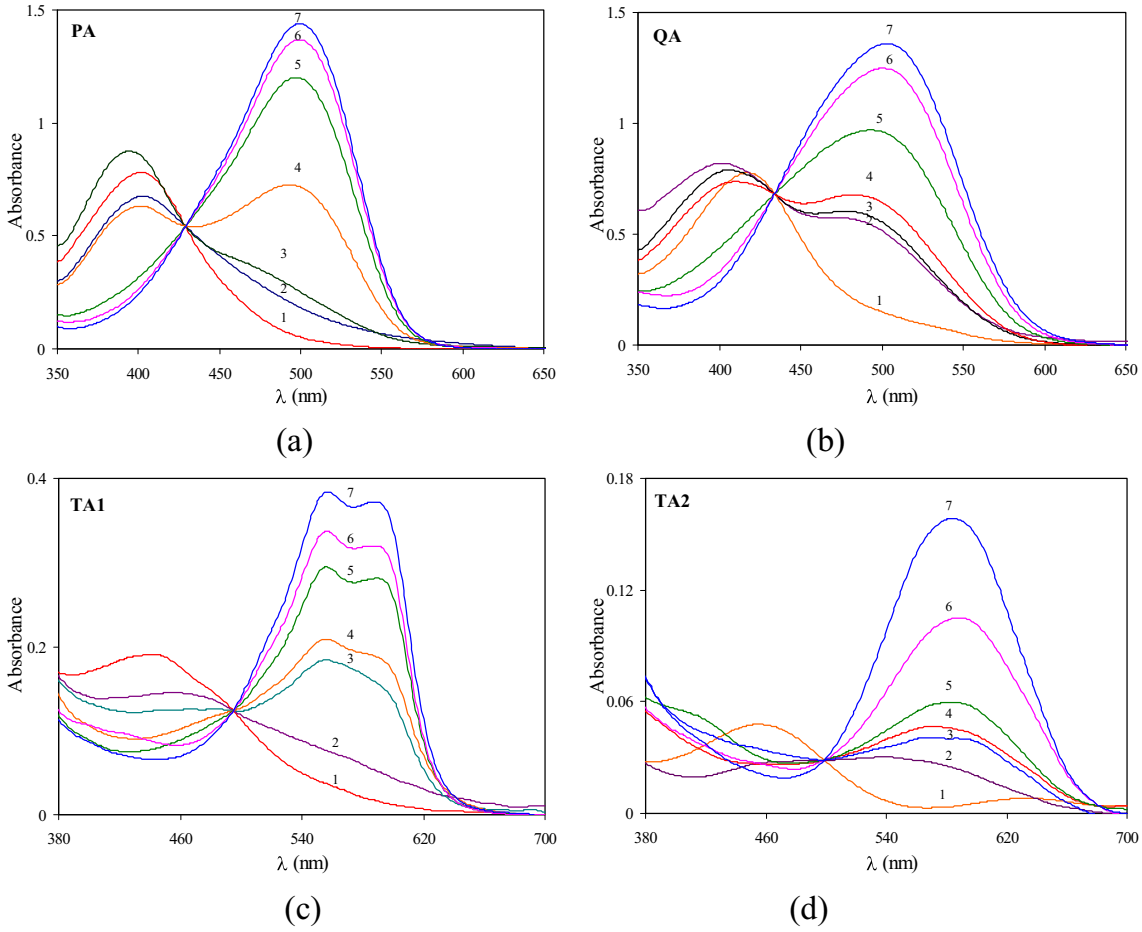

Fig. 9. Absorption spectra of the heteroarylazo quinoline dyes, (a) pyridylazo (PA), (b) quinolylazo (QA), (c) benzothiazolylazo-1 (TA1), and (d) benzothiazolylazo-2 (TA2) in various pH values; (1) pH = 1.1, (2) pH = 4, (3) pH = 7, (4) pH = 8, (5) pH = 9.1, (6) pH = 10.2, (7) pH = 13.2.

assumed to be partitioned in two regions [45,46]. The region in which a solute particle is surrounded by a solvation shell of solvent molecules is the local region, whereas, solvent molecules in bulk region are outside of the solvation shell. The maximum energy of absorption E_{12} of the solute depends on the composition of solvent mixture in the solvation shell; it can be related to the local mole fractions of the solvents as follows

$$E_{12} = x_1^l E_1 + x_2^l E_2 \quad (7)$$

where x_1^l and x_2^l represent the local mole fractions of the solvents 1 and 2 and $\sum_1 x_i^l = 1$.

Preferential solvation (PS) of the studied dyes was studied in the three mixed solvent systems including the hydrogen bond acceptor (HBA) and the hydrogen bond donor (HBD) components. The binary mixed solvents were (DMF-acetic acid), (DMSO-MeOH), and (toluene-MeOH) systems.

3.4.1. DMF-acetic acid binary system

Fig. 5a exhibits the influence of acetic acid (AA) on E_{12} values for PA in its mixture with DMF. As can be seen a positive deviation is observed in all the composition of the binary mixture, which indicates that the dye is solvated preferentially by a solvent having a higher transition energy value. Therefore, PA dye is preferentially solvated by AA. Fig. 5d

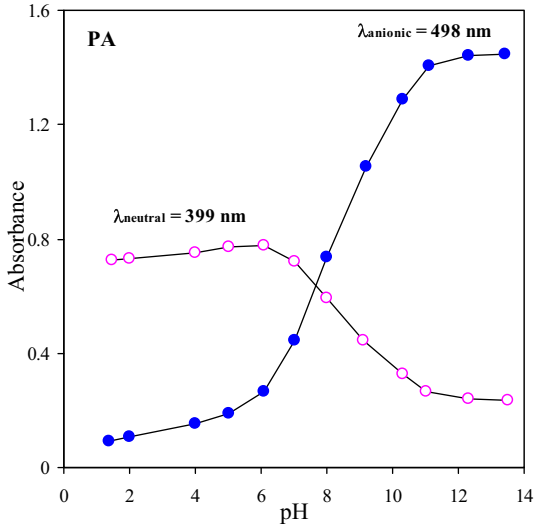

Fig. 10. Absorbance-pH curves for PA at $\lambda_{neutral}$ = 399 nm and $\lambda_{anionic}$ = 498 nm.

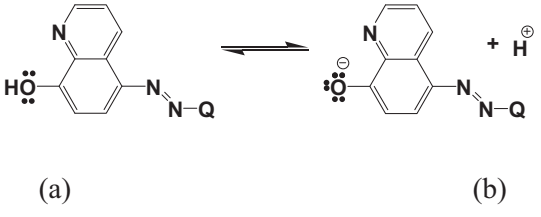

Fig. 11. Dissociation equilibrium of the heteroarylazo quinoline compounds (Structure of the (a) neutral and (b) anionic forms of the dyes).

Table 6
Ionization constants (pK_a) and absorption maxima (λ_{max}) of the azoquinoline dyes in different pH values.

Dye	λ_{max}nm (acidic)	λ_{max}nm (basic)	pK_a
Pyridylazo (PA)	399	498	7.30
Quinolylazo (QA)	414	502	7.26
Benzothiazolylazo (TA1)	439	556, 591	6.99
Benzothiazolylazo (TA2)	452	584	7.15

shows that the value of E_{12} for QA increases as AA is added to DMF up to $x_2 = 0.5$. It means that QA is preferentially solvated by DMF up to this mole fraction. However with increase in mole fraction of AA the value of E_{12} decreases and QA is preferentially solvated by AA. Existence of both the positive and negative deviation might be due to the dye-solvent and solvent-solvent interactions through the hydrogen bonding.

3.4.2. DMSO–MeOH binary system

The variation of E_{12} values in binary mixture containing methanol and DMSO along with the ideal lines are given in Fig. 5 (b,e). It shows that the experimental data deviate considerably from the ideal line. The solvation data indicates that both PA and QA preferentially solvated by DMSO over the entire composition range. This reflects the fact that methanol is an associated liquid through the hydrogen-bond and dipole-dipole interactions. In contrast, DMSO is very low associated liquid with a Kirkwood factor of g = 1.13 [47]. Therefore, DMSO molecules are able to solvate PA and QA dyes through hydrogen bonding and other electrostatic interactions.

Toluene–MeOH binary system: For both the dyes, a negative deviation is observed for toluene + methanol binary system. Fig. 5 (c,f) shows the plot of the E_{12} versus the mole fraction of the cosolvent (x_2). These plots exhibit that the E_{12} values of both the dyes decrease as methanol is added to toluene. The solvation data indicates that the dyes are preferentially solvated by methanol.

The benzothiazolyl azo dyes (TA1 and TA2) exist mainly in hydrazone forms in polar protic and polar aprotic solvents. However, their absorption spectra are very sensitive to small amounts sodium hydroxide solution, leading to the bands appearing at shorter wavelengths. They are mainly found in the anionic forms in media with alkaline nature. Therefore, this work presents the preferential solvation of benzothiazolyl azo dyes (hydrazone forms) in toluene-MeOH and DMSO-MeOH solvent mixtures. Fig. 6 exhibits a set of plots of E_{12} values for TA1 and TA2 as a function of methanol mole fraction for DMSO–MeOH and toluene–MeOH binary solvent systems.

In the case of DMSO–MeOH system, the plots show that the E_{12} values of the dyes decrease as methanol is added to DMSO, which indicate that the dyes are preferentially solvated by the dipolar aprotic solvent rather than methanol (Fig. 6 a and c). As methanol is a hydrogen-bonded structured liquid, the DMSO molecules are freer to interact with the dyes molecules. For the toluene - MeOH mixture the deviation of the observed E_{12} value from the ideal data is perfectly clear. Fig. 6 (b and d) shows the plots of E_{12} as a function of mole fraction of the protic solvent along with the ideal lines. The plots indicate that the dyes are preferentially solvated by methanol rather than toluene.

3.5. Estimation of the dipole moments

In this work, various nonpolar, dipolar aprotic, and polar protic solvents were used to record the absorption and emission spectra at room temperature. Typical emission spectra in chosen solvents for QA and TA2 are shown in Fig. 7 (a,b).

Usually azo dyes have no fluorescence properties due to deep suppressed effect of azo bridge [48]. Moreover, the presence of some substituents such as chlorine and bromine substituent causes also the fluorescence to be quenched. Therefore, there are little reports on fluorescent azo dyes are in the literature [48–50]. However, various azo dyes can exhibit fluorescence behaviour in appropriate condition such as existence of azo-hydrazone tautomerism. In general, influence of various

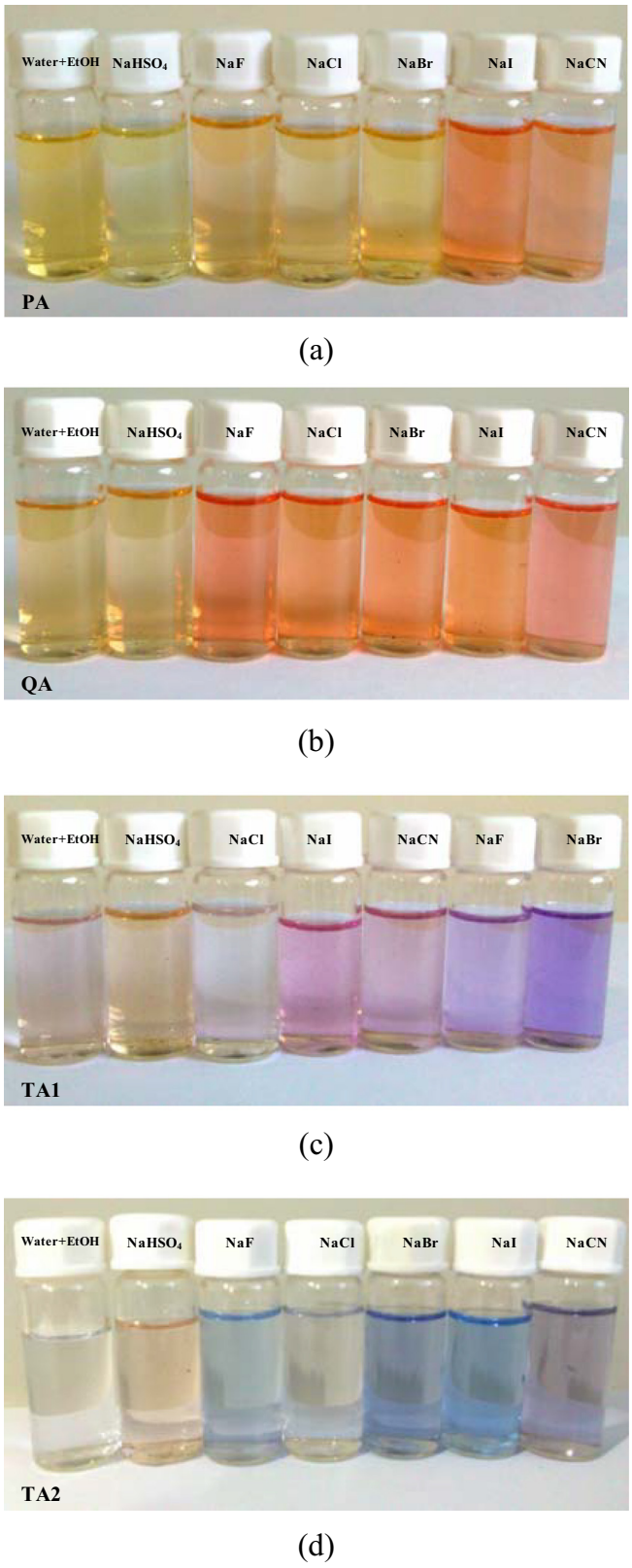

Fig. 12. Color change of (a) pyridylazo (PA), (b) quinolylazo (QA), (c) benzothiazolylazo-1 (TA1), (d) benzothiazolylazo-2 (TA2) with anions.

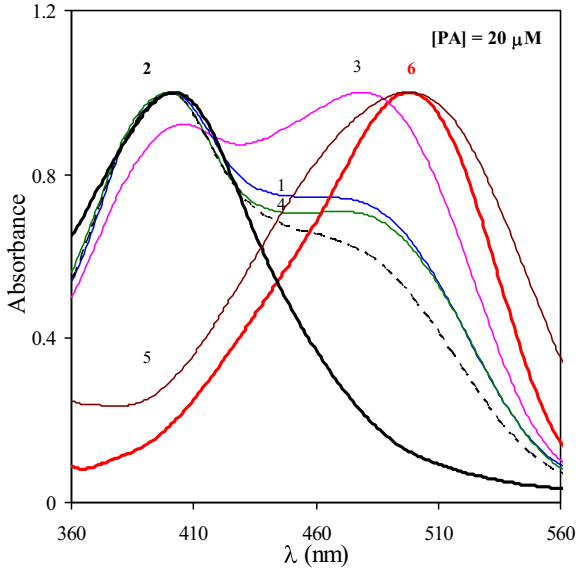

(a)

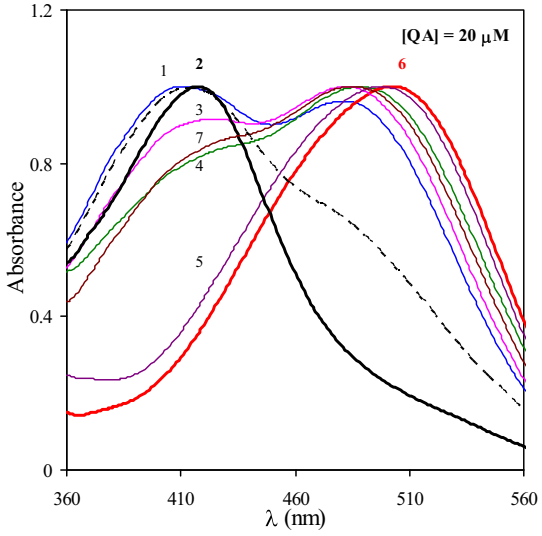

(b)

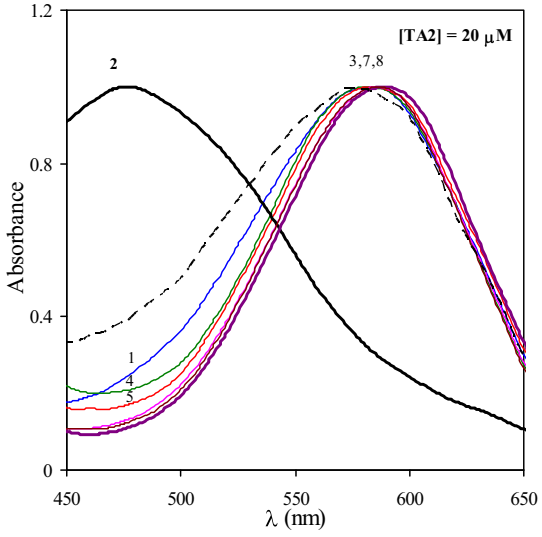

(c)

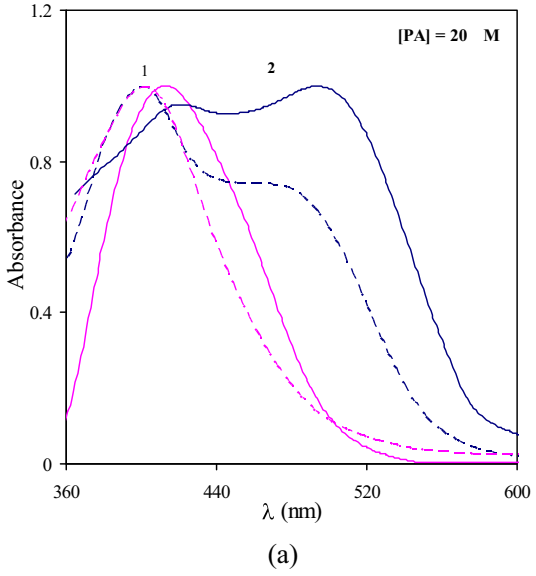

(a)

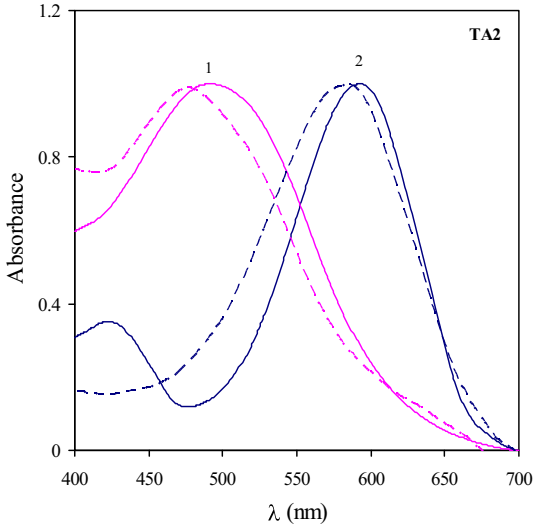

(b)

Fig. 14. Normalized absorption spectra of (a) pyridylazo (PA), (b) benzothiazolylazo-2 (TA2) in (1) $[BMIM]HSO_4$ and (2) [BMIM]Cl (dashed spectra is the absorbance of the dye in $NaHSO_4$ and NaCl solutions.

factors such as structure and aromatic components of dye molecules, the nature of substituents, ring closure, concentration, environment nature, self-association process, should be considered in the fluorescence properties of azo dyes. The studied azo dyes having heteroaryl moiety exhibit fluorescence properties in highly polar solvents. This property may come from hydrazone form of dyes. However, the fluorescence intensity is weak due to the presence of azo groups.

In order to determine the ground (μ_g) and excited states dipole moments (μ_e) of the dyes, the Lippert–Mataga, Bakhshiev, and Kawski-Chamma-Viallet methods were used. In estimation of the dipole moments, proper selected sets of solvents, which provide the best fit for the correlations, were used. The details of the methods and procedure used based on absorption and fluorescence shifts in various solvents have been reported in our previous publication [51]. The calculated ground and excited states dipole moments are given in Table 5. Typical

Fig. 13. Normalized absorption spectra of (a) pyridylazo (PA), (b) quinolylazo (QA), (c) benzothiazolylazo-2 (TA2) upon addition of (1) NaCl, (2) $NaHSO_4$, (3) NaBr, (4) NaF, (5) $NaHCO_3$, (6) NaCN (7) $NaCH_3COO$ (8) NaI (dashed spectrum is the absorbance of the dye in water-ethanol solution.).

Table 7
Dichroic ratios and degree of anisotropies obtained for the dyes in nematic liquid crystal (5CB).

Dye	$R = A_{II}/A_{\perp}$	$S_{dye} = (R-1)/(R+2)$
Pyridylazo (PA)	1.56	0.16
Quinolylazo (QA)	1.36	0.11
Benzothiazolylazo (TA1)	1.41	0.12
Benzothiazolylazo (TA2)	1.44	0.13

data associated to PA and QA dyes (in azo form) and TA1 (in hydrazone form) correlated with the solvent polarity functions are demonstrated in Fig. 8 (a−c).

As can be seen from the table, for each dye, the μ_e is larger than the μ_g due to relatively large electron density displacement in a more polar excited-state. Thus, the solute–solvent interactions can be stronger in the excited state than in the ground state. The calculated dipole moment data are approximately comparable and the used functions have acceptable correlation coefficients. However, the difference observed between the μ_e values can be explained in terms of different theoretical consideration used in development of these functions. In addition, effect of proper selected set of solvents used for each one of these theories should be considered.

3.6. Halochromism

Halochromism is a color change caused by a change in pH. In order to investigate the influence of pH on the spectral properties of the studied dyes, their absorption characteristics in 50 vo1% ethanol-water buffer solutions were studied over the pH range 1–13. The presence of the neutral and ionic species in solutions caused by the alkaline media can be involved in the spectral data of the dyes. The acid dissociation constants for the studied dyes were obtained using spectral analysis at a constant dye concentration and in 50% ethanol-water mixture (v/v).

As evident from Fig. 9 (a–d), these compounds, except compound TA1, display two absorption bands in the regions of short and long visible wavelengths for molecular and the anionic species, respectively. The TA1 dye shows three bands in the regions of 439, 556, and 591, which suggest the presence of one more species in the alkaline medium. The absorption bands show halochromic behavior. The intensity of the short-wavelength band decreases with increasing of pH up to pH = 13 and that of the latter band increases. The resulting spectrophotometric absorbance titration curve (absorbance as a function of pH) is typically shown in Fig. 10.

It is observed that only the anionic form exist at the highest pH recorded. This phenomenon suggests that the dye deprotonation process occurs in the most cases rather than tautomerism in the high alkaline media (Fig. 11). Table 6 summarizes the pK_a values of the compounds, which were calculated by the spectral analysis. For the dyes containing the benzothiazolyl groups, the pK_avalues show that the acidity of the hydroxyl group increases, while for the quinolyl and pyridyl dyes the acidic character decrease.

3.7. Anion affinity

The absorption spectral behavior of the dyes in aqueous-ethanol salt solutions (0.2 M) was studied as a function of the anion type. In this work, 12 different sodium salts including CH_3COONa, NaF, NaCl, NaBr, NaI, NaCN, $NaHCO_3$, $NaNO_3$, $NaNO_2$, Na_2HPO_4, $NaHSO_3$ and $NaHSO_4$ were used. Analyses of the spectral data provide information about anion affinity of the dye in solution. The change of color associated with the presence of some ionic species is typically shown in Fig. 12.

The spectral changes of the dyes ($C_{dye} = 2 \times 10^{-5}$ M) upon addition of the selected sodium salts are typically shown in Fig. 13. The absorption spectra of PA and QA in 50% water-ethanol solution without salt exhibit the dual bands due to the azo and hydrazone tautomers Fig. 13 (a, b). The spectral observation shown in Fig. 13c indicates that the TA2 exists in the hydrazone form in the water-ethanol solution. As evidenced from the figure, intensity of the long-wavelength bands, which belongs to the hydrazone tautomer, increase differently by addition of the various ions to the water-ethanol solutions. However, for all the studied dyes this process is reversed in the case of $NaHSO_4$. The observed short-wavelength band assigned to the azo tautomer is totally dominated in presence of acidic species HSO_4^-. In contrast, the hydrazone form is the only tautomer which is dominated in presence of sodium cyanide with the basic species.

On the other hand, addition of anions produced significant shifts in $\lambda_{max(hydrazone)}$. As can be seen from Fig. 13(a–c), the long-wavelength bands of the dyes belong to the hydrazone species red shifted in the order of $CN^- > HCO_3^- \geq CH3COO^- \geq I^- > Br^- > Cl^-$. The aqueous-ethanolic solutions of pyridylazo (PA) and quinolylazo (QA) dyes in presence of CN^- with formation of a reddish-orange color show the

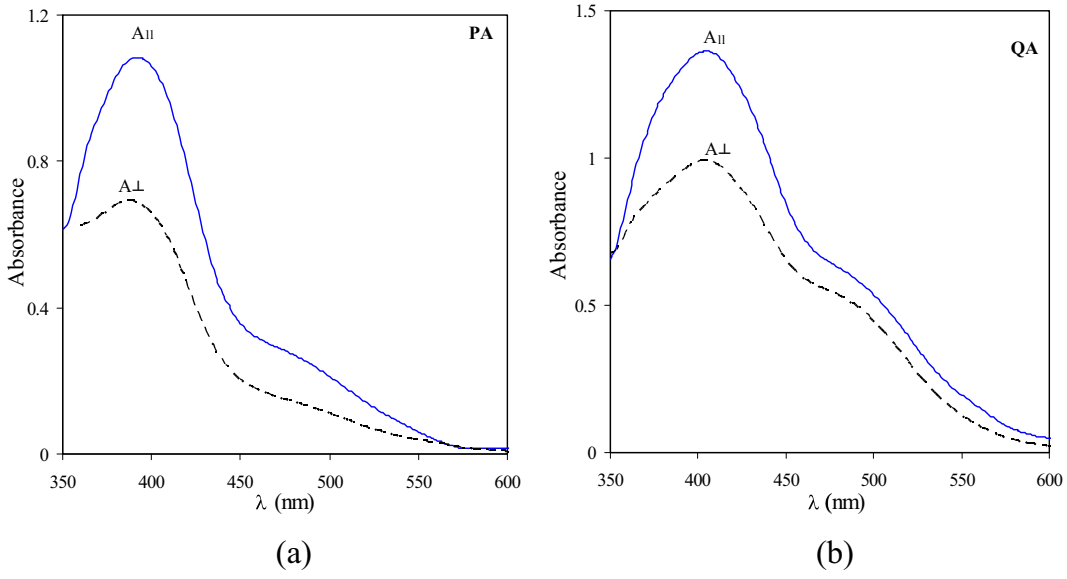

Fig. 15. Polarized absorption spectra of the heteroarylazo quinoline dyes (a) pyridylazo (PA), (b) quinolylazo (QA), in nematic liquid crystal of 5CB.

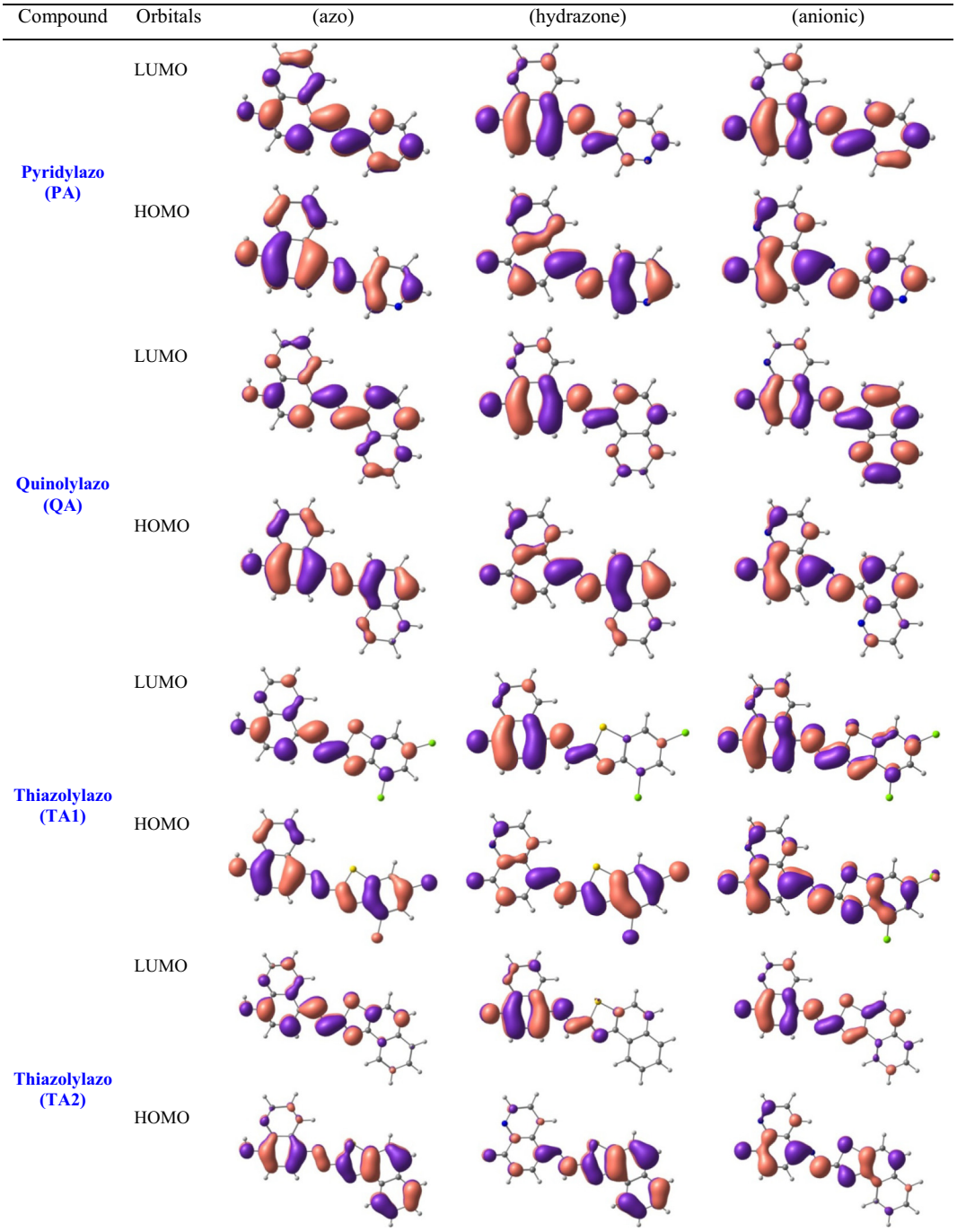

Fig. 16. The HOMO and LUMO distribution patterns of the heteroarylazo quinoline dyes.

maximum red shift. The similar trend was observed in the case of benzothiazolyl dyes (TA1 and TA2) but with formation of a purple color.

In this research, in order to elucidate the influence of liquid salts on the spectral and tautomeric behavior of the dyes, two room temperature imidazolium-based ionic liquids ([BMIM]Cl and [BMIM]HSO_4) were used as solvents. Typically, the absorption spectra of the dyes at a fixed dye concentration (2×10^{-5} M) in the pure ionic liquid solvents are plotted in Fig. 14 (a,b). As evidenced from the figure, similar spectral features are observed for the dyes in the ionic liquid and in their corresponding salts with the same anions. However, the spectral shift could be due to different contour ions and the possible interaction between $[BMIM]^+$ and the dye molecules.

3.8. Dichromism

The linear dichroism or absorption anisotropy ($A_{11} - A_{\perp}$) of a compound is defined as the difference in absorbance between two linearly polarized light possessing electric vectors perpendicular to each other. Polarized spectral data provide significant information on degree of orientational order of the dye molecules, the direction of the transition moments, and the polarization of electronic absorption bands [36].

The polarized absorption spectra of the heteroarylazo dyes dissolved in a parallel-aligned nematic liquid crystal (pentyl cyanobiphenyl) were measured using an optical cell with a 50 μm thickness. The dichroic ratios ($R = A_{\parallel}/A_{\perp}$) of the dyes were obtained by measuring the polarized

Table 8
The calculated electronic absorption spectral and dipole moment data for the azo, hydrazone and anionic forms of heteroarylazo quinoline dyes.

Compound	Solvent	λ_1 (azo) nm	λ_2 (hydrazone) nm	λ_3 (anionic) nm
Pyridylazo (PA)	Gas	396 [3.79]	399 [4.89]	433 [6.32]
	DMSO	413 [5.15]	425 [7.41]	457 [9.98]
	Acetic acid	412 [4.82]	422 [6.78]	455 [9.11]
Quinolylazo (QA)	Gas	426 [3.52]	436 [8.93]	534 [10.34]
	DMSO	446 [5.04]	472 [12.69]	515 [15.87]
	Acetic acid	444 [4.65]	466 [11.83]	520 [14.60]
Benzothiazolylazo (TA1)	Gas	446 [5.07]	437 [2.68]	457 [8.23]
	DMSO	472 [7.07]	450 [4.35]	492 [11.62]
	Acetic acid	469 [6.60]	448 [3.91]	488 [10.82]
Benzothiazolylazo (TA2)	Gas	494 [2.76]	354,504 [5.50]	484 [10.26]
	DMSO	519 [4.05]	360, 522 [7.80]	524 [14.76]
	Acetic acid	516 [3.70]	360, 520 [7.26]	517 [13.78]

The values in brackets are for dipole moments (Debye).
See Fig. 1 for the geometrical orientations of the molecules.

absorbances at λ_{max}. The order parameter of each dye was determined using the equation $S_{dye} = (A_{II} - A_{\perp})/(A_{II} + 2A_{\perp})$ [52]. The data from dichroism results are summarized in Table 7.

In general, the dye order parameter or degree of anisotropy is a function of the difference between the principal solute polarizabilities ($\Delta\alpha = 2\alpha_{zz} - \alpha_{xx} - \alpha_{yy}$). The presence of the bulky groups in the azo skeleton increases the polarizability of the molecules along three principal axes, which cause $\Delta\alpha$ and consequently S_{zz} decreases. According to the dichroism results, the dichroic ratios of the dyes are larger than one. This means that the absorption bands for these dyes may be considered as $\pi - \pi^*$. Typically, the polarized absorption spectra of the pyridyl and quinolyl azo dyes (PA and QA) dissolved in pentyl cyanobiphenyl (5CB) are shown in Fig. 15. It can be seen that the order parameter values of the dyes were found to be low and the difference between them are small. This is a consequence of the presence of bulky, pyridyl, quinolyl, and thiazolyls groups.

3.9. DFT and TD-DFT calculations

The time-dependent density functional theory (TD-DFT) calculations were performed and conducted to rationalize the observed spectroscopic data. First, we were optimized three forms including azo, hydrazone and minus ion for each of dye **1–4** to obtain the minimum energy structures at the B3LYP/6-31G* density functional theory (DFT) level [53]. Second, we were calculated wavelengths for the maximum absorption in the gas and two different solvents including DMSO and acetic acid by performing time-dependent (TD-DFT) calculations [54]. Distribution patterns for the highest occupied and the lowest unoccupied molecular orbitals (HOMO and LUMO) were also evaluated (Fig. 16). Our results indicated that the absorptions are influenced by the structural changes and also the solvents.

For PA and QA, the maximum absorptions were shifted to higher wavelengths from azo to ionic form whereas there is not such designated order for TA1 and TA2. Carefully comparing the absorption wave lengths could reveal that the maximum energies for transitions are required for azo forms of structures and the minimum energies are required for the anion form. However, the maximum energy is required for the hydrazone form of TA1 and the first absorption of TA2. Although the solvents have their effects on transitions, but the orders of changes are similar for all solvents from azo to anion forms. Examining the HOMO and LUMO distribution patterns indicates that the transitions could be mainly considered as $\pi \rightarrow \pi^*$ transitions. There is a significant point for hydrazone form of TA2, in which there are two sharp absorption peaks for this structure whereas those of others are all single peak absorption. Changes the values of dipole moments have been also observed for the compounds in different forms and media (Table 8). We did not expect to obtain the exact magnitudes of experiments by calculations, but the magnitudes of wavelengths for the maximum absorptions are almost in similar ranges for both of computational and experimental observations.

4. Conclusions

In this research, four heteroarylazo quinoline dyes were synthesized and characterized by standard analytical methods. This study presents the photophysical and structural characteristics of the newly synthesized dyes with different substituents in various solvents. The solvatochromism, azo-hydrazone tautomerism, halochromism, dichroism, anion affinity, and preferential solvation of the compounds were studied by electronic spectroscopy in various media. The existence of azo-hydrazone tautomerism was supported by UV–vis and ^{1}H NMR spectral studies in addition to fluorescence and theoretical investigations.

The solvatochromism of the dyes in pure solvents was analyzed with the Kamlet-Taft and Katritzky LSER models, which indicate that it is affected largely by the dipolarity/polarizability of the solvent. Moreover, the experimental results suggest that the media basicity and molecular structure of the dyes are essential factors to solvatochromic and azo-hydrazone tautomeric properties. The spectral and tautomeric behavior in the mixed binary solvents including DMF-acetic acid, DMSO-methanol, and toluene-methanol was analyzed using the preferential solvation method. In DMSO-methanol system, the free alcohol molecules become less available for solvation due to the strong self-association through hydrogen bond and dipole-dipole interactions. In contrast, in toluene-methanol binary mixture, the dyes are preferentially solvated by methanol. In the case of DMF-acetic acid mixture, the pyridylazo dye is preferentially solvated by acetic acid in all the composition of the binary mixture, while the quinolylazo dye is preferentially solvated by DMF at mole fraction 0.5, then the dye is preferentially solvated by acetic acid. The acid dissociation constants (pK_a) of the dyes were measured using their absorption spectral data. The existence of the neutral and anionic species in the buffer solutions of varying pH was involved in the spectra of the dyes. The halochromism results indicate that the anionic form occurs easily at the high alkaline media, suggesting that the dye deprotonation process preferential occurs rather than tautomerism.

It was found that the spectral behavior of azo and hydrazone tautomers was shifted by the use of sodium salts. The dyes reported in this research show that their photophysical behavior is sensitive to anions such as CN ion. According to the linear dichroism measurements, positive dichroic ratios are obtained for the studied dyes in a nematic host. Thus, all the absorption bands are due to the $\pi - \pi^*$ transitions (parallel transition). The Lippert–Mataga, Bakhshiev, and Kawski$^-$Chamma^{--} Viallet equations were used to calculate the ground and excited states dipole moments of the compounds. As a result, the dipole moments in the excited state are larger than the ground state for all the dye

molecules. The calculated dipole values are almost comparable and the equations have acceptable correlation coefficients.

To support the spectroscopic and structural characterization of the compounds, theoretical computations were carried out by the B3LYP/6-31G* method and the electronic transitions and structural properties were explained with the theoretical treatment.

Acknowledgments

The authors thank the university authorities for providing the necessary facilities to carry out the work.

Appendix A. Supplementary data

Supplementary data to this article can be found online at https://doi.org/10.1016/j.molliq.2018.10.054.

References

[1] M.A. Rauf, S. Hisaindee, J. Mol. Struct. 1042 (2013) 45–56.
[2] I. Sener, F. Karcı, N. Ertan, E. Kılıc, Dyes Pigments 70 (2006) 143–148.
[3] J. Geng, Y. Dai, H.F. Qian, N. Wang, W. Huang, Dyes Pigments 117 (2015) 133–140.
[4] U. Warde, N. Sekar, Dyes Pigments 137 (2017) 384–394.
[5] Z. Seferoglu, N. Ertan, T. Hokelek, E. Sahin, Dyes Pigments 77 (2008) 614–625.
[6] E. Aktan, N. Ertan, T. Uyar, J. Mol. Struct. 1060 (2014) 215–222.
[7] H.F. Qian, Z. Xiao-Lei, Y. Dai, W. Huang, Dyes Pigments 143 (2017) 223–231.
[8] J. Chen, Zh. Yin, Dyes Pigments 102 (2014) 94–99.
[9] A. Saylam, Z. Seferoglu, N. Ertan, Dyes Pigments 76 (2008) 470–476.
[10] A. Ghanadzadeh Gilani, M. Moghadam, M.S. Zakerhamidi, E. Moradi, Dyes Pigments 92 (2012) 1320–1330.
[11] A. Saylam, Z. Seferoğlu, N. Ertan, J. Mol. Liq. 195 (2014) 267–276.
[12] Ö. Arslan, B. Aydıner, E. Yalçın, B. Babür, N. Seferoğlu, Z. Seferoğlu, J. Mol. Struct. 1149 (2017) 499–509.
[13] M.S. Masoud, A.E. Ali, M.A. Shaker, M.A. Ghani, Spectrochim. Acta A 60 (2004) 3155–3159.
[14] B. Babur, N. Seferoglu, E. Aktan, T. Hokelek, E. Sahin, Z. Seferoglu, J. Mol. Struct. 1081 (2015) 175–181.
[15] P. Ball, C.H. Nicholls, Dyes Pigments 3 (1982) 5–26.
[16] M.A. Rauf, S. Hisaindee, N. Saleh, RSC Adv. 5 (2015) 18097–18110.
[17] P.G. Umape, V.S. Patil, V.S. Padalkar, K.P. Phatangare, V.D. Gupta, A.B. Thate, N. Sekar, Dyes Pigments 98 (2013) 507–517.
[18] D. Debnath, S. Roy, B.H. Li, C.H. Lin, T.K. Misra, Spectrochim. Acta A 140 (2015) 185–197.
[19] A. Ghanadzadeh Gilani, E. Moradi, S. Binay, M. Moghadam, Spectrochim. Acta A 82 (2012) 112–118.
[20] A.S. Shawali, J. Adv. Res. 1 (2010) 255–290.
[21] L. Antonov, S. Kawauchi, M. Satoh, J. Komiyama Dyes, Pigments 40 (1999) 163–170.
[22] E.O. Moradi Rufchahi, A. Ghanadzadeh Gilani, V. Taghvaei, R. Karimi, N. Ramezanzade, J. Mol. Struct. 1108 (2016) 623–630.
[23] Q. Peng, M. Li, K. Gao, L. Cheng Dyes, Pigments 18 (1992) 271–286.
[24] A.S. Özen, P. Doruker, V. Aviyente, J. Phys. Chem. A 111 (2007) 13506–13514.
[25] A. Unal, B. Eren, E. Eren, J. Mol. Struct. 1049 (2013) 303–309.
[26] A.S. Choudhari, S.R. Patil, N. Sekar, Color. Technol. 132 (2016) 1–12.
[27] A. Ghanadzadeh Gilani, V. Taghvaei, E.O. Moradi Rufchahi, M. Mirzaei, Spectrochim. Acta A 185 (2017) 111–124.
[28] A. Ghanadzadeh Gilani, M. Moghadam, M.S. Zakerhamidi, Dyes Pigments 92 (2012) 1052–1057.
[29] A. Ghanadzadeh Gilani, M. Salmanpour, T. Ghorbanpour, J. Mol. Liq. 179 (2013) 118–123.
[30] E. Lippert, Z. Elektrochem. 61 (1957) 962–975.
[31] N.G. Bakhshiev Opt, Spektrosk. 16 (1964) 821–832.
[32] A. Chamma, P. Viallet, C.R. Acad. Sci. C270 (1970) 1901–1904.
[33] C. Reichardt, Solvents and Solvent Effects in Organic Chemistry, Third edition Wiley-VCH, 2003.
[34] T. Bevilaqua, T.F. Goncalves, C.G. Venturini, V.G. Machado, Spectrochim. Acta A 65 (2006) 535–542.
[35] G. Meier, E. Sackmarm, J.G. Grabmaier, Application of Liquid Crystals, Springer-Verlag, Berlin, Heidelberg, 1975.
[36] J. Michl, E.W. Thulstrup, Spectroscopy with Polarized Light Wiley-VCH Book, 1995.
[37] R.G. Bares, V.E. Bower, Anal. Chem. 28 (1956) 1322–1324.
[38] L.G. Van Uitert, C.G. Haas, J. Am. Chem. Soc. 75 (1953) 451–455.
[39] A. Ghanadzadeh Gilani, S. Shokri, J. Mol. Liq. 193 (2014) 194–203.
[40] C. Schmidt, G. Schmidt-Naake, Macromol. Mater. Eng. 292 (2007) 1164–1175.
[41] A. Ghanadzadeh Gilani, M. Moghadam, S.E. Hosseini, J. Mol. Liq. 231 (2017) 27–38.
[42] A.R. Katritzky, D.C. Fara, H. Yang, K. Tamm, T. Tamm, M. Karelson, J. Chem. Rev. 104 (2004) 175–198.
[43] D.C. Silva, I. Ricken, M.A. Silva, V.G. Machado, J. Phys. Org. Chem. 15 (2002) 420–427.
[44] O.A. Adegoke, Spectrochim. Acta A 83 (2011) 504–510.
[45] T. Bevilaqua, T.F. Goncalves, C.G. Venturini, V.G. Machado, Spectrochim. Acta A 65 (2006) 535–542.
[46] A.K. Laha, P.K. Das, S. Bagchi, J. Phys. Chem. A 106 (2002) 3230–3234.
[47] A. Ghanadzadeh Gilani, M. Moghadam, T. Ghorbanpour, J. Chem. Thermodyn. 113 (2017) 263–275.
[48] P.P. Kasture, Y.A. Sonawane, R.N. Rajule, G.S. Shankarling, Synthesis and characterisation of benzothiazole-based solid-state fluorescent azo dyes, Color. Technol. 126 (2010) 348–352.
[49] M.A. Satam, R.K. Raut, R.D. Telore, N. Sekar, Fluorescent acid azo dyes from 3-(1,3-benzothiazol-2-yl)naphthalen-2-ol and comparison with 2-naphthol analogs, Dyes Pigments 97 (2013) 32–42.
[50] U. Warde, N. Sekar, NLOphoric mono-azo dyes with negative solvatochromism and in-built ESIPT unit from ethyl 1,3-dihydroxy-2-naphthoate: estimation of excited state dipole moment and pH study, Dyes Pigments 137 (2017) 384–394.
[51] A. Ghanadzadeh Gilani, S.E. Hosseini, M. Moghadam, E. Alizadeh, Spectrochim. Acta A 89 (2012) 231–237.
[52] A. Ghanadzadeh, M.A. Shahzamanian, S. Shoarinejad, M.S. Zakerhamidi, M. Moghadam, J. Mol. Liq. 136 (2007) 22–28.
[53] M.J. Frisch, G.W. Trucks, et al., Gaussian 09, Revision A.01, Gaussian, Inc., Wallingford CT, 2009.
[54] www.chemcrftprog.com.